Mn doped InSb studied at the atomic scale by cross-sectional scanning tunneling microscopy

Mn doped InSb studied at the atomic scale by cross-sectional scanning tunneling microscopy

S. J. C. Mauger,[1] J. Bocquel,[1] P. M. Koenraad,[1,a)] C. E. Feeser,[2] N. D. Parashar,[2] and B. W. Wessels[2]
[1]*Department of Applied Physics, Eindhoven University of Technology, Den Dolech 2, 5612 AZ Eindhoven, The Netherlands*
[2]*Department of Materials Science and Engineering and Materials Research Center, Northwestern University, Evanston, Illinois 60208, USA*

(Received 13 September 2015; accepted 13 November 2015; published online 30 November 2015)

We present an atomically resolved study of metal-organic vapor epitaxy grown Mn doped InSb. Both topographic and spectroscopic measurements have been performed by cross-sectional scanning tunneling microscopy (STM). The measurements on the Mn doped InSb samples show a perfect crystal structure without any precipitates and reveal that Mn acts as a shallow acceptor. The Mn concentration of the order of $\sim 10^{20}\,\mathrm{cm}^{-3}$ obtained from the cross-sectional STM data compare well with the intended doping concentration. While the pair correlation function of the Mn atoms showed that their local distribution is uncorrelated beyond the STM resolution for observing individual dopants, disorder in the Mn ion location giving rise to percolation pathways is clearly noted. The amount of clustering that we see is thus as expected for a fully randomly disordered distribution of the Mn atoms and no enhanced clustering or second phase material was observed. © *2015 AIP Publishing LLC*. [http://dx.doi.org/10.1063/1.4936754]

Dilute magnetic semiconductors (DMS) have attracted a strong scientific interest in recent years. Such materials can combine electrical, optical, and magnetic properties that can be applied, for instance, in information processing.[1,2] On the road to achieve room temperature applications, the highest Curie temperature (T_C) for DMS has been predicted for transition metal dopants in wide gap semiconductors. However, transition metal dopants in wide gap semiconductors form deep levels in the band gap, leading to reduced conductivity. Additionally, the formation of defects in the host material, such as As antisites and Mn interstitials in (Ga,Mn)As, reduces the carrier concentration and lowers the carrier mediated ferromagnetism.[3] Interestingly, high Curie temperatures have been achieved for narrow gap (III,Mn)V semiconductors grown by metal-organic vapor epitaxy (MOVPE) with $T = 330\,\mathrm{K}$ for (In,Mn)As[4,5] and more than $T = 400\,\mathrm{K}$ for (In,Mn)Sb,[6] despite the prediction of a low T_C by mean field theory for DMS.[3] The position of the Mn acceptor level in narrow gap III–V semiconductors is predicted to be either shallow or resonant in the valence band, and narrow gap III–V semiconductors have the advantage to remain highly conductive even for a high Mn concentration and therefore should allow for desired high temperature magnetic properties.[7]

In this paper, we present an atomically resolved study of (In,Mn)Sb by cross-sectional Scanning Tunneling Microscopy (X-STM)[8,9] to determine the structural and electronic properties of this material. The electronic state and related incorporation site of the magnetic Mn atoms, the formation of clusters and second phases as well as the formation of additional defects are all important for a full understanding of the properties of (In,Mn)Sb. X-STM is an excellent technique to explore such properties. It is also interesting to measure with X-STM the distribution of the magnetic atoms in the material. For instance, it was shown that percolation can play an important role in the Curie temperature of ferromagnetic materials.[10,11] Furthermore, theoretical calculations have shown that disorder in the distribution of the magnetic dopant atoms in dilute magnetic semiconductors such as atomic scale clusters and dopant pair formation can lead to an increase of the Curie temperature.[12] Such atomic scale clustering has been suggested to be involved in the ferromagnetism observed in (In,Mn)As.[13] Another approach that deals with a possible spatial disorder in the distribution of Mn atoms is proposed by Kennett *et al.*[11] They developed a two-component-model whereby disorder in the Mn ion locations can lead to spatially inhomogeneous local magnetizations that are strongly correlated with the local charge density. Thus, the incorporation of transition metal dopant atoms and their distribution can play a central role in determining the magnetic properties of the DMS. The question arises as to the nature of the dopant disorder at concentrations of the order of $\sim 10^{20}\,\mathrm{cm}^{-3}$. X-STM is well-suited to reveal the dopant distribution at high resolution.[9,14–16] No spatial study at the atomic scale of Mn:InSb has yet been reported. Here we show that Mn is incorporated on the group III site and acts as a shallow acceptor and that no additional defects were observed. Interestingly, we found that the dopant distribution is fully uncorrelated for pair distances beyond 3 nm. However, local disorder, as is to be expected for an uncorrelated pair distribution function, is observed in the X-STM images of ionized Mn acceptors in (In,Mn)Sb and no indications were found for enhanced clustering or second phases.

The InSb films doped with Mn were grown by MOVPE on an undoped InSb substrate at a temperature of $T = 400\,^{\circ}\mathrm{C}$. The film thickness of our samples is 500 nm and the Mn

a)p.m.koenraad@tue.nl

concentration measured by Energy Dispersive X-ray Spectroscopy (EDX) is $9 \times 10^{19}\,\mathrm{cm}^{-3}$. Please note that the uncertainty in this value can be rather high because the data are taken close to the detection limit of this technique. Temperature dependent resistivity measurements show that the samples exhibit a metallic-like conduction, which is consistent with the Mott limit indicating a critical hole composition of $2.4 \times 10^{17}\,\mathrm{cm}^{-3}$. SQUID magnetometry performed at different temperatures on samples with a similar doping level and grown under similar conditions as the sample that has been studied by X-STM showed a clear magnetic hysteresis at room-temperature.

For the X-STM measurements, the samples were cleaved *in situ* along their natural (110) cleavage plane under ultra high vacuum conditions ($P < 4 \times 10^{-11}$ mbar), and the measurements were performed at 77 K using a commercial Omicron scanning tunneling microscope. In a very large number of scans taken at different positions in the epilayer and the substrate, we do always find a perfect single zinc-blende phase with no evidence for a second phase or any (nano)clustering. A typical large scale atomically resolved X-STM image of the (In,Mn)Sb (110) cleavage surface obtained at constant current and positive sample voltage (empty state imaging) is shown in Fig. 1. The bright features correspond with substitutional Mn acceptors at different depths below the cleavage surface. In previous X-STM measurements on (Mn,Ga)As, we were able to prove that Mn acts as an deep acceptor that incorporates on a group III site as an Mn^{2+} ion with a $3d^5$ ground state.[8] Depending on the polarity of the applied voltage, either the neutral or ionized charge state of the Mn acceptor is imaged. This is due to tip-induced band bending which can pull the Mn acceptor level below the Fermi level at a negative voltage bringing the Mn acceptor into an ionized state, whereas at positive sample voltage, the acceptor level of the Mn dopant can be pulled above the Fermi level bringing the acceptor into a neutral state. In Fig. 1, which is taken at positive sample voltage, we observe the Mn acceptors in their neutral state and the Scanning Tunneling Microscopy (STM) contrast of a single Mn reflects the charge distribution of the hole bound to the Mn acceptor. This is in excellent agreement with X-ray Absorption Spectroscopy that indicated the presence of Mn^{2+} ions with a $3d^5$ ground state, corresponding with an acceptor-like behavior, in similar MOVPE grown InSb samples. Previous STM studies on various acceptors with a different binding energy in III–V semiconductors have shown that the charge distribution of the hole bound to the acceptor is related to the binding energy of the acceptor.[8,17] At a fixed depth, the charge distribution of a deep acceptor (binding energy of the order of 100 meV or more) is characterized by a bow-tie shape[8,17] whereas the shape of the charge distribution of a shallow acceptor, such as Zn in GaAs[18] or Mn in InAs,[19] is triangular. Our X-STM measurements clearly show a triangular contrast for the Mn dopants corresponding with a shallow acceptor state. This agrees with the study of Obukhov *et al.*,[20] where it is shown that Mn in InSb acts as a shallow acceptor with a binding energy of about 9 meV.[21,22] If we image the cleaved surface at negative voltages (filled state imaging) we observe circular symmetric contrast. For Mn in GaAs we know that the acceptor at these tunnel conditions is ionized due to the band bending.[8,23] The circular symmetric contrast is thus due to the influence of the Coulomb potential of the ionized Mn acceptor on the tunneling process.

The differences in the shape and intensity of the Mn contrast observed in Fig. 1 is related to the depth of Mn atoms below the (110) surface.[24] Fig. 2(b) shows the

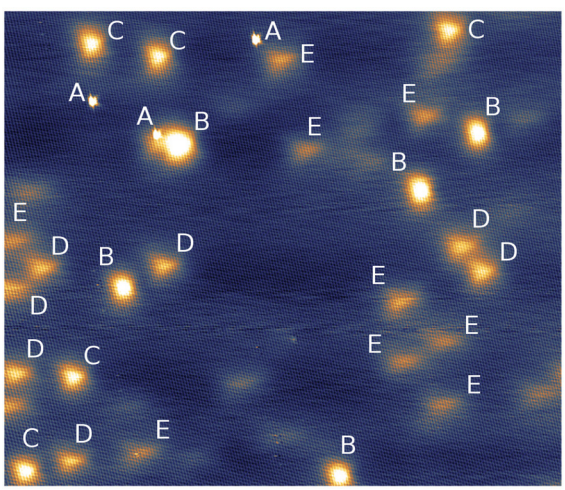

FIG. 1. Constant current X-STM topographic image (100 nm × 85 nm) of the (110) Mn:InSb surface. The indices correspond with the depth of the Mn acceptor below the (110) surface ($V_{sample} = +0.5$ V and I = 50 pA).

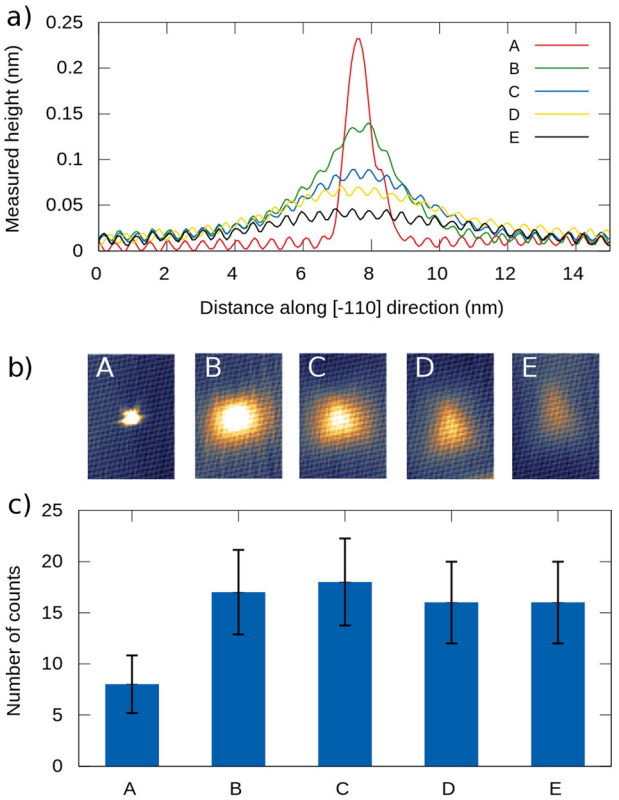

FIG. 2. (a) Topographic profile lines along the [110] direction for the various classes of Mn acceptors in InSb observed under the same tunnel conditions as in Fig. 1. All these Mn acceptors are in their neutral charge state configuration under these tunnel conditions. (b) Constant current STM images (10 nm × 7 nm) of the same classes of Mn acceptors observed under the same tunnel conditions. (c) Histogram of the number of Mn acceptors of each class observed in Fig. 1.

different classes of contrast of Mn acceptors that can be found in Fig. 1. The highly localized feature of class A in Fig. 2(b) corresponds to an Mn acceptor localized in the uppermost monolayer of InSb. The contrasts B-E all have an almost triangular shape but the intensity of the contrast varies strongly as shown by the profile lines taken in the 110 direction and shown in Fig. 2(a). The Mn impurities with a less intense contrast are located deeper below the (110) cleavage plane than the impurities with a more intense contrast. Thus, we conclude that the acceptors of class B-C-D-E are located, respectively, in the 2nd, 3rd, 4th, and 5th monolayer below the (110) surface. Because Mn acceptors deeper below the cleavage surface are not resolved as clearly and distinctively as those in layer 1–5, they are not categorized. Fig. 2(c) shows the frequency distribution of the different classes of Mn contrast. The frequency of appearance is homogeneous for every class of Mn contrast except for the Mn in the uppermost layer which appears less than the other classes. The frequency of the Mn acceptors in the top five layers was used to determine the Mn doping concentration. The estimated Mn concentration based on the X-STM measurement shown in Fig. 1 is 3×10^{19} cm^3, which is somewhat lower than that obtained from EDX measurements (9×10^{19} cm^3) on this sample. This difference is very likely due to the uncertainties in: (1) the EDX measurements where the data are obtained close to their detection limit, (2) the uncertainty in the counting based on the X-STM measurements, and (3) a gradient in the Mn concentration that we observed in this sample. Because we cleave the sample along the growth direction we get a cross-section through the grown epilayers and the substrate and thus various regions of the epilayer and the substrate have been scanned. While scanning the (110) plane in the [001] direction from the epilayer towards the substrate, no clear (In,Mn)Sb/InSb interface was found. Instead we observe a monotonous decrease of the Mn concentration extending from the epilayer into the substrate. Mn atoms have been found at a distance of up to 1500 nm from the top of the film. Because the Mn:InSb epilayer thickness is 500 nm, Mn atoms must have diffused by 1000 nm into the substrate. The small difference between the melting point of InSb (527 °C) and the growth temperature (400 °C) might be related to this long range diffusion.

The sample was also analyzed by X-STM spectroscopy. In these measurements the feedback loop of the piezo-scanner is deactivated and at each point in the studied area the current is measured while the voltage is scanned. Fig. 3 shows the *dI/dV* spectra taken on a free InSb (110) surface (red line) and on an Mn impurity (blue line). The current at negative sample voltage is due to the electrons tunneling from the filled states of the sample (i.e., valence band) to the tip whereas at positive sample voltage, the current is due to the electrons tunneling from the tip into the empty states (i.e., conduction band). The band gap of InSb, at the measurement temperature of 77 K, can be determined from the range of low tunnel current and is about 0.3 eV. This is a good agreement with the value of 0.23 eV at 80 K that is reported in the literature. When no voltage is applied between the semiconductor sample and the STM tip, the Fermi levels of the tip and the semiconductor are aligned. We can thus conclude from the spectroscopy measurements

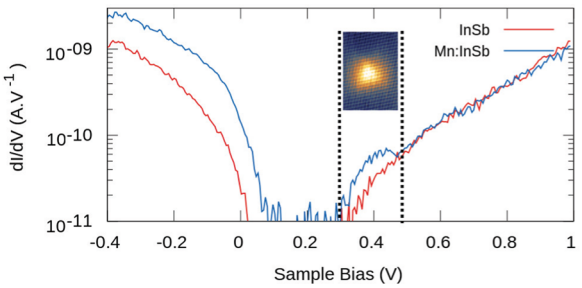

FIG. 3. Local tunneling spectroscopy spectra measured on Mn:InSb obtained with the set point at $V_{sample} = +1$ V and I = 200 pA. The red line represents the *dI/dV* spectra on the free InSb (110) surface whereas the blue line represents the *dI/dV* spectra taken on an Mn acceptor. The inset shows an empty state X-STM image of an Mn acceptor in InSb obtained at $V_{sample} = +0.5$ V and I = 50 pA.

that the semiconductor Fermi level is located close to the top of the valence band, which is to be expected for p-type material and further supports our conclusion that Mn acts as an acceptor in InSb.

The spectroscopy measurements on an Mn atom show an extra current channel at about 0.4 V, which is due to the electrons tunneling from the STM tip into the neutral acceptor state. At these tunnel conditions, the appearance of the triangular contrast is best observed. The additional current at negative sample voltage measured at the position of an Mn acceptor is due to the influence of the Coulomb potential of the ionized Mn acceptor on the tunnel current.

In order to determine the disorder of the spatial distribution of the Mn atoms in the InSb sample, we used a filled state image mode ($V_{sample} = -0.8$ V and I = 200 pA) at which mainly Mn atoms in the outermost surface layer are detected, see Fig. 4(a). At these tunnel conditions, the Mn atoms are observed in their ionized state, which allows for an optimal spatial resolution of about 3 nm (see inset in Fig. 4(b)). We used an automated procedure to determine the position of each Mn atom in the image (marked by a black star) and from these dopant positions the radial distribution function was derived (Fig. 4(b)). The value of the radial distribution function is close to unity for all distances beyond 3 nm, proving that the Mn-distribution is purely random at these length scales. The amount of disorder and clustering that we see is thus as is expected for a fully randomized distribution of Mn doping atoms. The dip in the radial distribution below 3 nm is due to the X-STM technique, which does not allow to separate two neighboring Mn atoms that are closer to each other than the resolution limit under these tunnel conditions. If we image the surface at positive voltage, when the Mn atoms are in their neutral state, we can recognize close pairs more easily.[9] However, we did not observe any indication that excessive Mn-pairing, as was for instance found to occur in (In,Mn)As,[13] is taking place in our (In,Mn)Sb sample.

The image in Fig. 4(a) shows topographic contrast, i.e., the tip is retracted due to an enhanced tunneling probability, around each ionized Mn atom. This topographic contrast is at maximum 50 pm and extends laterally over about 3 nm. The height contrast we observe in Fig. 4(a) is due to a spatial variation in the integrated density-of-states, which is available for tunneling from the semiconductor to the tip, i.e., the total density-of-states that is present in the energy range

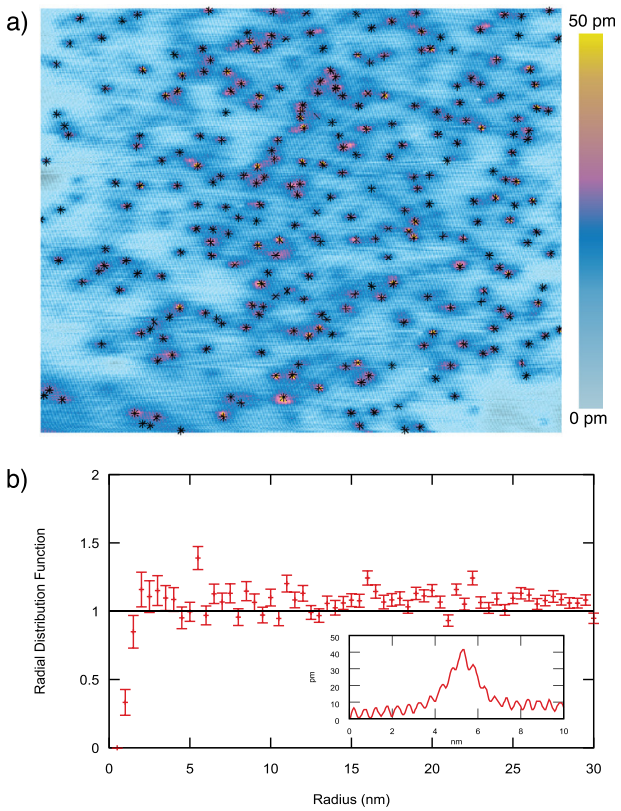

FIG. 4. (a) Filled state X-STM topography (100 nm × 100 nm) of ionized Mn acceptors (black stars) near the (110) InSb surface. ($V_{sample} = -0.8$ V and I = 200 pA) The topographic contrast extends over 50 pm and is represented by a color scale where yellow corresponds with the tip retracted furthest away from the surface. (b) Radial distribution function of the Mn acceptors observed in (a). Inset: Topographic profile line along the [110] direction of an Mn acceptor in InSb observed in Fig. 4(a) in its ionized charge state.

between the top of the valence band and the tip Fermi-level. The contrast varies because the local Coulomb potential around each charged acceptor (the Mn atoms are ionized at the applied tunnel condition) is not constant. This will locally shift the top of the valence band.[23] Because the tip is operating in a constant current mode, the height of the tip (the topographic contrast) is adjusted such that the tunnel current remains constant when more states become available for tunneling. In the present case, the tip is retracted when the energy interval over which electrons can be extracted from the valence band locally increases due to a variation in the local Coulomb potential. The dark blue regions in the topographic are thus attributed to the effect of the local Coulomb potential from the ionized Mn acceptor. It appears that the areas with enhanced contrast, the dark blue regions which correspond with a higher local electrostatic potential, are forming interconnected networks of local potential variations. The holes, donated by the Mn-acceptors, will modify their spatial distribution according to the local potential network and form conductive percolation pathways through the InSb matrix. Along such pathways, stronger interactions between the (magnetic) ions might occur, but it is difficult to estimate how much this will exactly affect the magnetic behavior. It remains thus of high interest to explore further the role of disorder in the distribution of magnetic acceptors, considering both the role of the spatial location of the magnetic moments and the related percolating network of the carriers that can be involved in coupling the magnetic moments.

In conclusion, the incorporation of Mn and its spatial distribution in diluted, magnetic semiconductor (In,Mn)Sb was investigated by X-STM. It was found that Mn atoms incorporate as Mn^{2+} ions and thus act as a well-behaved acceptor. The observed contrast of neutral Mn atoms agrees with a small binding energy for the hole bound to this acceptor. The impurities are randomly distributed for pair distances greater than 3 nm, which is the resolution limit of our approach. The amount of clustering that we see at a doping concentration of the order of $\sim 10^{20}$ cm^{-3} is thus as expected for a fully randomly disordered distribution, and no indications were found for enhanced pairing or enhanced clustering of the Mn on a short length scale or the formation of second phase inclusions. Well-resolved percolation pathways associated with the Coulomb potential of Mn acceptor are observed in the X-STM images. These pathways might be important for understanding the reported ferromagnetic behavior.

The research leading to these results has received funding from the European Community's Seventh Framework Programme (PF7/2007-2013) under Grant Agreement No. 215368 and from the United States Programmes NSF DMR-0804479 and DMR-1305666.

[1]H. Ohno, Science **281**, 951 (1998).
[2]Y. Ohno, D. K. Young, B. Beschoten, F. Matsukura, H. Ohno, and D. D. Awschalom, Nature **402**, 790 (1999).
[3]T. Dietl, H. Ohno, F. Matsukura, J. Cibert, and D. Ferrand, Science **287**, 1019 (2000).
[4]A. Blattner and B. Wessels, in *Papers from 29th Conference on the Physics and Chemistry of Semiconductor Interfaces* (2002), Vol. 20, p. 1582.
[5]A. Blattner, J. Lensch, and B. Wessels, J. Electron. Mater. **30**, 1408 (2001).
[6]N. D. Parashar, N. Rangaraju, V. K. Lazarov, S. Xie, and B. W. Wessels, Phys. Rev. B **81**, 115321 (2010).
[7]B. W. Wessels, New J. Phys. **10**, 055008 (2008).
[8]A. M. Yakunin, A. Y. Silov, P. M. Koenraad, J. H. Wolter, W. Van Roy, J. De Boeck, J. M. Tang, and M. E. Flatte, Phys. Rev. Lett. **92**, 216806 (2004).
[9]A. M. Yakunin, A. Y. Silov, P. M. Koenraad, J. M. Tang, M. E. Flatte, W. Van Roy, J. De Boeck, and J. H. Wolter, Phys. Rev. Lett. **95**, 256402 (2005).
[10]K. Sato, W. Schweika, P. H. Dederichs, and H. Katayama-Yoshida, Phys. Rev. B **70**, 201202(R) (2004).
[11]M. P. Kennett, M. Berciu, and R. N. Bhatt, J. Magn. Magn. Mater. **272**, 1993 (2004).
[12]G. Bouzerar, T. Ziman, and J. Kudrnovský, Appl. Phys. Lett. **85**, 4941 (2004).
[13]Y. L. Soo, S. Kim, Y. H. Kao, A. J. Blattner, B. W. Wessels, S. Khalid, C. Sanchez Hanke, and C. C. Kao, Appl. Phys. Lett. **84**, 481 (2004).
[14]D. Kitchen, A. Richardella, J.-M. Tang, M. E. Flatte, and A. Yazdani, Nature **442**, 436 (2006).
[15]A. Richardella, P. Roushan, S. Mack, B. Zhou, D. Huse, D. Awschalom, and A. Yazdani, Science **327**, 665 (2010).
[16]M. Bozkurt, A. Grant, J. M. Ulloa, R. P. Campion, C. T. Foxon, E. Marega, G. J. Salamo, and P. M. Koenraad, Appl. Phys. Lett. **96**, 042108 (2010).
[17]C. Celebi, J. K. Garleff, A. Y. Silov, A. M. Yakunin, P. M. Koenraad, W. Van Roy, J.-M. Tang, and M. E. Flatte, Phys. Rev. Lett. **104**, 086404 (2010).
[18]Z. F. Zheng, M. B. Salmeron, and E. R. Weber, Appl. Phys. Lett. **64**, 1836 (1994).

[19]F. Marczinowski, J. Wiebe, F. Meier, K. Hashimoto, and R. Wiesendanger, Phys. Rev. B **77**, 115318 (2008).
[20]S. A. Obukhov, B. S. Neganov, Y. F. Kiselev, A. N. Chemikov, V. S. Vekshina, N. I. Pepik, and A. N. Popkov, Cryogenics **31**, 874 (1991).
[21]S. A. Obukhov, Phys. Status Solidi B **242**, 1298 (2005).
[22]J. Teubert, S. A. Obukhov, P. J. Klar, and W. Heimbrodt, Phys. Rev. Lett. **102**, 046404 (2009).
[23]K. Teichmann, M. Wenderoth, S. Loth, R. G. Ulbrich, J. K. Garleff, A. P. Wijnheijmer, and P. M. Koenraad, Phys. Rev. Lett. **101**, 076103 (2008).
[24]J. K. Garleff, C. Celebi, W. Van Roy, J. M. Tang, M. E. Flatte, and P. M. Koenraad, Phys. Rev. B **78**, 075313 (2008).